Research in Astron. Astrophys. **2011** Vol. **11** No. **5**, 617–624
http://www.raa-journal.org *http://www.iop.org/journals/raa*

Research in Astronomy and Astrophysics

Instability of the cometary plasma tail — the instability in a plasma sheet *

Lin-Zhong Liu[1], Yue-Hua Ma[1,2] and Jian-Chun Shi[1,2]

[1] Purple Mountain Observatory, Chinese Academy of Sciences, Nanjing 210008, China
[2] National Astronomical Observatories, Chinese Academy of Sciences, Beijing 100012, China; *yhma@pmo.ac.cn*

Received 2010 March 31; accepted 2010 November 30

Abstract We consider the instability of the cometary plasma tail which is composed of a neutral sheet, two lobes of the ion tail and solar wind. The plasma is assumed to be highly conductive and incompressible. The unstable state yields a magnetic field which is perpendicular to the tail axis. Our result is consistent with findings about plasma from the International Cometary Explorer (ICE).

Key words: methods: analytical — comets: general

1 INTRODUCTION

In the 1950s, people started to investigate the interaction between solar wind and comets in order to understand the cometary magnetic field, plasma motion, structure and stability. Biermann (1951) predicted the existence of solar wind from studying the direction of cometary plasma tails. Alfvén (1957) proposed the concept of interplanetary magnetic fields. He considered that the formation of the cometary ionized layer and plasma tail is due to the solar wind blowing an interplanetary magnetic field into the cometary atmosphere. Biermann et al. (1967) found that a strong bow shock wave exists upstream of the cometary nucleus. Wallis (1971) suggested the shock wave could be weak.

In early research about the structure and stability of comets, the model used usually regarded the cometary ionized tail as a plasma cylinder (Ershkovich & Mendis 1986) and the related magnetohydrodynamic (MHD) effects were considered. The MHD waves are excited by the Kelvin-Helmholtz (K-H) instability. In the head of the comet, the contact plane of discontinuity (i.e. the ionopause) between pure cometary plasma and the polluted solar wind plasma is unstable (Ershkovich et al. 1986; Ershkovich & Flammer 1988; Ershkovich et al. 1989; Ershkovich & Israelevich 1993). Therefore, the interplanetary magnetic field wrapping around the cometary atmosphere can flow into the contact plane of discontinuity but not form a magnetic cavity (Ip & Axford 1990). After the discovery (Neubauer et al. 1986) of a magnetic field-free cavity around the nucleus of Comet Halley by the Giotto mission, Cravens (1986) and Ip & Axford (1987) have shown that such a magnetic field distribution might result from a balance between the magnetic force $\boldsymbol{J} \times \boldsymbol{B}$ and the neutral-ion drag. Ershkovich et al. (1989) have taken into account the effects of dissociative recombination and mass-loading arising from photoionization, and reached the conclusions that the Halley ionopause and its

* Supported by the National Natural Science Foundation of China.

adjacent ionospheric layer with a thickness of $\sim$100 km may possibly remain unstable, although the growth rate is substantially reduced due to recombination. The stability analysis by McKenzie et al. (1990) is extended to include the effects of finite plasma pressure; the results demonstrate that plasma pressure reduces the instability growth rate of the cavity. Then the stability analysis of a cometary ionosphere is extended to include the effects of plasma motion by Ershkovich & Israelevich (1993), where they arrive at the conclusion that the cometary ionopause cannot be at rest.

Since 1985, many spacecrafts have passed through cometary plasma tails and obtained many valuable data. The International Cometary Explorer (ICE) spacecraft flew through the plasma tail of Comet Giacobini-Zinner (G.-Z.) in 1985 and found a neutral region between two tail lobes (Slavin et al. 1986). In the neutral region, there was a magnetic field of 5 nT perpendicular to the direction of the tail. Neubauer (1990) proposed this was the interplanetary magnetic field penetrating into the head of the comet and the magnetic structure of the cometary head can be divided into four parts – from inner to outer: magnetic cavity region, magnetic pile-up region, magneto-sheath and upstream wave region, and they are separated by the interface ionopause, pile-up boundary and bow shock, respectively. If we extend this structure to a plasma tail, which can (at least) be divided into the middle region (neutral sheet), the magnetic pile-up region (i.e. the magnetic lobes of the tail) and the region surrounding the solar wind. The cometary plasma tail should be oblate instead of cylindrical, especially at the tail end (Wegmann 2002). However, the existence of the magnetic cavity region shows that the ionopause is stable. It is impossible for magnetic lines to penetrate into the head of the comet. We suggest that the magnetic field perpendicular to the direction of the tail is excited by plasma instability in the neutral region.

The ESA/NASA Ulysses spacecraft, which is in a polar orbit about the Sun, had unplanned encounters with the ion or plasma tails of at least three comets: C/1996 B2 (Hyakutake) (Gloeckler et al. 2000; Jones et al. 2000; Riley et al. 1998), C/1999 T1 (McNaught-Hartley) (Gloeckler et al. 2004), and C/2006 P1 (McNaught) (Neugebauer et al. 2007). Neugebauer et al. (2007) compared these cometary tail encounter events and found that the minimum velocity in the tail strongly depended on the distance of the spacecraft from the nucleus, indicating continued acceleration of the plasma down to the tail. In Comet Hyakutake, the velocity shear between the flow in the tail and that in the surrounding solar wind had nearly disappeared.

Recent research works have mostly used numerical methods (e.g. Hansen et al. 2007; Wegmann 2002) to simulate the plasma conditions resulting from the interaction between comets and the solar wind. However, those considering the stability of the cometary ionopause and oblate cometary plasma tail are very limited. We try to study this phenomenon to gain more insight into this problem.

In the model of Alfvén (1957) about the magnetic lines wrapping around the cometary atmosphere, the outline of the bundle of magnetic lines is like a bundle of parabolic curves whose focus is on the cometary nucleus. In this paper, we use a special mathematical model to solve this problem.

2 MATHEMATICAL MODEL

When studying the motion and stability of cometary plasma modeled by the MHD method, we use vector analysis in the differential form with exterior derivatives. This method can be partly found in books about general differential forms (e.g. Westenholy 1981).

In a rectangular coordinate system, vector $\boldsymbol{A}$ can be expressed as three components

$$\boldsymbol{A} = A_x\boldsymbol{i} + A_y\boldsymbol{j} + A_z\boldsymbol{k}, \tag{1}$$

where $\boldsymbol{i}, \boldsymbol{j}$ and $\boldsymbol{k}$ are three basic vectors of the rectangular coordinate system, respectively. With the differentiable manifold M being R^3, the cotangent space of a point P is $T{*}_p(M)$. In $T{*}_p(M)$, regarding 1-form as a vector, we have

$$\boldsymbol{A} = A_x dx + A_y dy + A_z dz, \tag{2}$$

where dx, dy and dz are basic vectors, respectively. Thereupon, elementary operations with differential forms can substitute for the operations in vector algebra and vector analysis. Here we have

$$\left.\begin{aligned} \boldsymbol{A}\cdot\boldsymbol{B} &= *(\boldsymbol{A}\wedge *\boldsymbol{B}) = *(*\boldsymbol{A}\wedge\boldsymbol{B}) \\ \boldsymbol{A}\times\boldsymbol{B} &= *(\boldsymbol{A}\wedge\boldsymbol{B}) \end{aligned}\right\}, \tag{3}$$

where $*$ is Hodge's star operator and $\wedge$ is an exterior product (or wedge product) operator. In the rectangular coordinate system,

$$\left.\begin{array}{lll} *dx = dy\wedge dz, & *dy = dz\wedge dx, & *dz = dx\wedge dy, \\ *(dy\wedge dz) = dx, & *(dz\wedge dx) = dy, & *(dx\wedge dy) = dz, \\ *1 = dx\wedge dy\wedge dz, & *(dx\wedge dy\wedge dz) = 1, & ** = 1. \end{array}\right\} \tag{4}$$

In the general orthogonal curve coordinate system, the coordinate of a point P is (q^1, q^2, q^3). The length of an arc is

$$ds^2 = h_1^2(dq^1)^2 + h_2^2(dq^2)^2 + h_3^2(dq^3)^2, \tag{5}$$

where the natural basis of local coordinates is (dq^1, dq^2, dq^3), the orthogonal basis is $(\boldsymbol{e}^1 = h_1 dq^1, \boldsymbol{e}^2 = h_2 dq^2, \boldsymbol{e}^3 = h_3 dq^3)$, and h_1, h_2 and h_3 are Lamé coefficients.

In the local orthogonal basis, a vector $\boldsymbol{A}$ can be written in component form as

$$\boldsymbol{A} = A_1\boldsymbol{e}^1 + A_2\boldsymbol{e}^2 + A_3\boldsymbol{e}^3 = A_i\boldsymbol{e}^i, \tag{6}$$

where the same superscript and subscript i denote the sum from 1 to 3 for i (i.e., the Einstein summation convention).

From Equation (3), the main formulae for the associated vector analysis are

$$\left.\begin{aligned} \mathrm{div}\boldsymbol{A} &= \nabla\cdot\boldsymbol{A} = *(\nabla\wedge *\boldsymbol{A}) \\ \mathrm{rot}\boldsymbol{A} &= \nabla\times\boldsymbol{A} = *(\nabla\wedge\boldsymbol{A}) \end{aligned}\right\}, \tag{7}$$

where ∇ is the Hamiltonian operator. We find continued operators $\nabla\wedge$ which is just the exterior differential operator d. Then we have

$$\left.\begin{aligned} \mathrm{div}\boldsymbol{A} &= *d*\boldsymbol{A} \\ \mathrm{rot}\boldsymbol{A} &= *d\boldsymbol{A} \\ \mathrm{gradf} &= df \end{aligned}\right\}, \tag{8}$$

where f is a differentiable function. Therefore we have

$$\left.\begin{aligned} \mathrm{div} &= *d* \\ \mathrm{rot} &= *d \\ \mathrm{grad} &= d \end{aligned}\right\}. \tag{9}$$

Using Equation (9) and the calculation rule of exterior differentiation, we can obtain the following formulae for vector analysis:

$$\mathrm{grad}(fg) = d(fg) = gdf + fdg = g\,\mathrm{grad}f + f\,\mathrm{grad}g,$$

$$\mathrm{rot}(f\boldsymbol{A}) = *d(f\boldsymbol{A}) = *[df\wedge\boldsymbol{A} + fd\boldsymbol{A}] = (\mathrm{grad}f)\times\boldsymbol{A} + f\,\mathrm{rot}\boldsymbol{A},$$

$$\mathrm{div}(f\boldsymbol{A}) = *d*(f\boldsymbol{A}) = *[df\wedge *\boldsymbol{A} + fd*\boldsymbol{A}] = (\mathrm{grad}f)\cdot\boldsymbol{A} + f\mathrm{div}\boldsymbol{A},$$

$$\begin{aligned} &\mathrm{div}(\boldsymbol{A}\times\boldsymbol{B}) = *d**(\boldsymbol{A}\wedge\boldsymbol{B}) = *d(\boldsymbol{A}\wedge\boldsymbol{B}) = *[(d\boldsymbol{A})\wedge\boldsymbol{B} - \boldsymbol{A}\wedge d\boldsymbol{B}] \\ &= *[**(d\boldsymbol{A})\wedge\boldsymbol{B} - \boldsymbol{A}\wedge **d\boldsymbol{B}] = (\mathrm{rot}\boldsymbol{A})\cdot\boldsymbol{B} - \boldsymbol{A}\cdot\mathrm{rot}\boldsymbol{B}, \end{aligned}$$

$$\mathrm{rot}(\mathrm{grad}f) = *d(df) = *ddf = 0,$$
$$\mathrm{div}(\mathrm{rot}\boldsymbol{A}) = *d**d\boldsymbol{A} = *dd\boldsymbol{A} = 0.$$

By the calculation rule of the exterior differential

$$d\boldsymbol{e}^i = -\omega_j^i \wedge \boldsymbol{e}^j, \tag{10}$$

where ω_j^i are 1-forms of Cartan connection forms, so we have

$$\begin{aligned}\nabla \times \boldsymbol{A} &= \nabla \times (A_i \boldsymbol{e}^i) = *d(A_i \boldsymbol{e}^i) = *[dA_i \wedge \boldsymbol{e}^i + A_i d\boldsymbol{e}^i] \\ &= *[dA_j \wedge \boldsymbol{e}^j + A_i(-\omega_j^i) \wedge \boldsymbol{e}^j] = *[(dA_j - A_i\omega_j^i) \wedge \boldsymbol{e}^j] = *[(DA_j) \wedge \boldsymbol{e}^j],\end{aligned} \tag{11}$$

where $DA_j = dA_j - A_i\omega_j^i$, namely Liu's operator, which is a covariant differential of a covariant vector field A_j. Now we get the Liu's arithmetic result as follows

$$\left.\begin{aligned}\mathrm{rot}(A_i\boldsymbol{e}^i) &= \nabla \times (A_i\boldsymbol{e}^i) = (DA_i) \times \boldsymbol{e}^i \\ \mathrm{div}(A_i\boldsymbol{e}^i) &= \nabla \cdot (A_i\boldsymbol{e}^i) = (DA_i) \cdot \boldsymbol{e}^i \\ (\boldsymbol{A}_i \cdot \nabla)\boldsymbol{B} &= (\boldsymbol{A} \cdot \nabla)B_i\boldsymbol{e}^i = (\boldsymbol{A} \cdot DB_i)\boldsymbol{e}^i \\ Df &= df = \mathrm{grad}f\end{aligned}\right\}, \tag{12}$$

where the formula

$$\begin{aligned}2(\boldsymbol{A} \cdot \nabla)\boldsymbol{B} &= \mathrm{rot}(\boldsymbol{B} \times \boldsymbol{A}) + \mathrm{grad}(\boldsymbol{A} \cdot \boldsymbol{B}) + \boldsymbol{A}\mathrm{div}\boldsymbol{B} \\ &- \boldsymbol{B}\mathrm{div}\boldsymbol{A} - \boldsymbol{A} \times \mathrm{rot}\boldsymbol{B} - \boldsymbol{B} \times \mathrm{rot}\boldsymbol{A},\end{aligned} \tag{13}$$

has been used. The following formulae are also obtained

$$\begin{aligned}\mathrm{rot}(\boldsymbol{A} \times \boldsymbol{B}) &= \nabla \times (A_iB_j\boldsymbol{e}^i \times \boldsymbol{e}^j) = D(A_iB_j) \times (\boldsymbol{e}^i \times \boldsymbol{e}^j) \\ &= [(DA_i)B_j + A_i(DB_j)] \times (\boldsymbol{e}^i \times \boldsymbol{e}^j) = (DA_i) \times (\boldsymbol{e}^i \times \boldsymbol{B}) + (DB_j) \times (\boldsymbol{A} \times \boldsymbol{e}^j) \\ &= (\boldsymbol{B} \cdot DA_i)\boldsymbol{e}^i - \boldsymbol{B}[(DA_i) \cdot \boldsymbol{e}^i] + \boldsymbol{A}[(DB_j) \cdot \boldsymbol{e}^j] - (\boldsymbol{A} \cdot DB_j)\boldsymbol{e}^j \\ &= (\boldsymbol{B} \cdot \nabla)\boldsymbol{A} - \boldsymbol{B}\mathrm{div}\boldsymbol{A} + \boldsymbol{A}\mathrm{div}\boldsymbol{B} - (\boldsymbol{A} \cdot \nabla)\boldsymbol{B},\end{aligned}$$

$$\begin{aligned}\mathrm{grad}(\boldsymbol{A} \cdot \boldsymbol{B}) &= D(A_iB_j\boldsymbol{e}^i \cdot \boldsymbol{e}^j) = (DA_i)(\boldsymbol{e}^i \cdot \boldsymbol{B}) + (DB_j)(\boldsymbol{A} \cdot \boldsymbol{e}^j) \\ &= \boldsymbol{B} \times (DA_i \times \boldsymbol{e}^i) + (\boldsymbol{B} \cdot DA_i)\boldsymbol{e}^i + \boldsymbol{A} \times (DB_j \times \boldsymbol{e}^j) + (\boldsymbol{A} \cdot DB_j)\boldsymbol{e}^j \\ &= \boldsymbol{B} \times \mathrm{rot}\boldsymbol{A} + (\boldsymbol{B} \cdot \nabla)\boldsymbol{A} + \boldsymbol{A} \times \mathrm{rot}\boldsymbol{B} + (\boldsymbol{A} \cdot \nabla)\boldsymbol{B}.\end{aligned}$$

In the general orthogonal curve coordinate system, we have

$$\mathrm{div}\boldsymbol{A} = *d*(A_i\boldsymbol{e}^i) = \frac{1}{h_1h_2h_3}\Big(\frac{\partial A_1h_2h_3}{\partial q^1} + \frac{\partial A_2h_3h_1}{\partial q^2} + \frac{\partial A_3h_1h_2}{\partial q^3}\Big),$$

$$\mathrm{rot}\boldsymbol{A} = *d(A_i\boldsymbol{e}^i) = \begin{bmatrix}\dfrac{\boldsymbol{e}^1}{h_2h_3} & \dfrac{\boldsymbol{e}^2}{h_3h_1} & \dfrac{\boldsymbol{e}^3}{h_1h_2} \\ \dfrac{\partial}{\partial q^1} & \dfrac{\partial}{\partial q^2} & \dfrac{\partial}{\partial q^3} \\ h_1A_1 & h_2A_2 & h_3A_3\end{bmatrix},$$

$$\begin{aligned}&(\boldsymbol{A} \cdot \nabla)\boldsymbol{B} = (\boldsymbol{A} \cdot \nabla))B_i\boldsymbol{e}^i = (\boldsymbol{A} \cdot DB_i)\boldsymbol{e}^i \\ &= \Big[\frac{A_1}{h_1}\Big(\frac{\partial B_1}{\partial q^1} + \frac{B_2}{h_2}\frac{\partial h_1}{\partial q^2} + \frac{B_3}{h_3}\frac{\partial h_1}{\partial q^3}\Big) + \frac{A_2}{h_2}\Big(\frac{\partial B_1}{\partial q^2} - \frac{B_2}{h_1}\frac{\partial h_2}{\partial q^1}\Big) + \frac{A_3}{h_3}\Big(\frac{\partial B_1}{\partial q^3} - \frac{B_3}{h_1}\frac{\partial h_3}{\partial q^1}\Big)\Big]\boldsymbol{e}^1 \\ &+\Big[\frac{A_2}{h_2}\Big(\frac{\partial B_2}{\partial q^2} + \frac{B_1}{h_1}\frac{\partial h_2}{\partial q^1} + \frac{B_3}{h_3}\frac{\partial h_2}{\partial q^3}\Big) + \frac{A_1}{h_1}\Big(\frac{\partial B_2}{\partial q^1} - \frac{B_1}{h_2}\frac{\partial h_1}{\partial q^2}\Big) + \frac{A_3}{h_3}\Big(\frac{\partial B_2}{\partial q^3} - \frac{B_3}{h_2}\frac{\partial h_3}{\partial q^2}\Big)\Big]\boldsymbol{e}^2 \\ &+\Big[\frac{A_3}{h_3}\Big(\frac{\partial B_3}{\partial q^3} + \frac{B_1}{h_1}\frac{\partial h_3}{\partial q^1} + \frac{B_2}{h_2}\frac{\partial h_3}{\partial q^2}\Big) + \frac{A_1}{h_1}\Big(\frac{\partial B_3}{\partial q^1} - \frac{B_1}{h_3}\frac{\partial h_1}{\partial q^3}\Big) + \frac{A_2}{h_2}\Big(\frac{\partial B_3}{\partial q^2} - \frac{B_2}{h_3}\frac{\partial h_2}{\partial q^3}\Big)\Big]\boldsymbol{e}^3.\end{aligned}$$

3 EQUATIONS AND SOLUTION

We suppose the plasma in the neutral sheet is highly conductive and incompressible. Considering the momentum coupling between the neutral molecules and the ions, the equation of motion is

$$\rho\Big[\frac{\partial \boldsymbol{V}}{\partial t}+(\boldsymbol{V}\cdot\nabla)\boldsymbol{V}\Big]=-\nabla\Phi+\frac{1}{4\pi}(\boldsymbol{B}\cdot\nabla)\boldsymbol{B}+\rho v_{\rm in}(\boldsymbol{V}_n-\boldsymbol{V}), \tag{14}$$

$$\frac{\partial \boldsymbol{B}}{\partial t}={\rm rot}(\boldsymbol{V}\times\boldsymbol{B})=(\boldsymbol{B}\cdot\nabla)\boldsymbol{V}-(\boldsymbol{V}\cdot\nabla)\boldsymbol{B}, \tag{15}$$

$$\nabla\cdot\boldsymbol{V}=\nabla\cdot\boldsymbol{B}=0, \tag{16}$$

where ρ, $\boldsymbol{V}$ and $\boldsymbol{B}$ denote the mass density, the bulk velocity and the magnetic field of plasma respectively; $\Phi=P+B^2/8\pi$ is the total pressure, v_{in} is collision frequency between the ions and the neutral molecules, and $\boldsymbol{V}_n$ is the velocity of the neutral gas. In the neutral sheet, $\boldsymbol{B}_0$ is equal to 0. We adopt the parabolic cylindrical coordinate system (Fig. 1). The coordinate curves are parabolas whose foci are located at the cometary nucleus (Liu 1999). We have

$$\left.\begin{aligned} x &= c(\alpha^2-\beta^2)/2,\\ y &= c\alpha\beta,\\ z &= z, \end{aligned}\right\} \tag{17}$$

with the origin of the Cartesian coordinate system located at the nucleus, the *ox* axis directed toward the Sun and the *oxy* plane in the ecliptic plane. Here (α,β,z) are the parameters of parabolic cylindrical coordinates, and *c* is the factor of length.

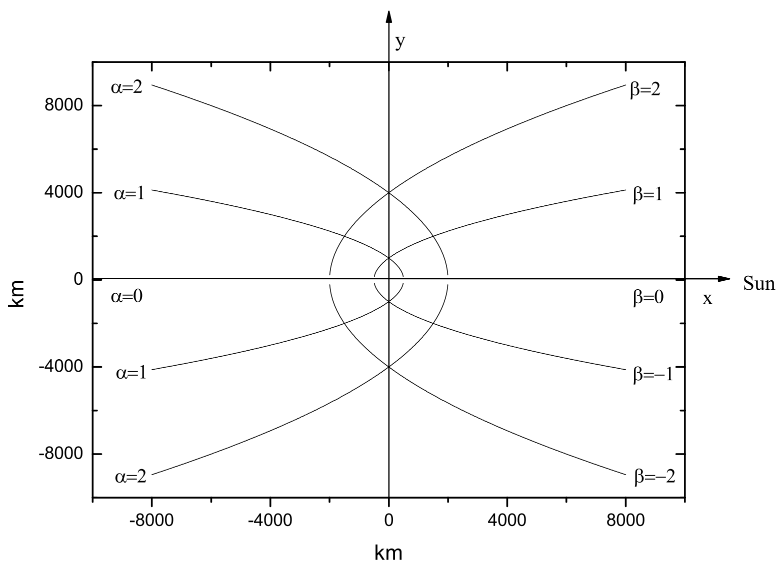

Fig. 1 Sketch of parabolic cylindrical coordinates with $c=1000$ km.

The small perturbation equation is

$$\rho\Big[\frac{\partial \boldsymbol{v}}{\partial t}+(\boldsymbol{v}\cdot\nabla)\boldsymbol{V}_0\Big]=-\nabla\varphi+\frac{1}{4\pi}(\boldsymbol{B}_0\cdot\nabla)\boldsymbol{b}-\rho v_{\rm in}\boldsymbol{v}, \tag{18}$$

$$\frac{\partial \boldsymbol{b}}{\partial t}=(\boldsymbol{b}_0\cdot\nabla)\boldsymbol{v}-(\boldsymbol{b}\cdot\nabla)\boldsymbol{V}_0-(\boldsymbol{v}\cdot\nabla)\boldsymbol{B}_0-(\boldsymbol{V}_0\cdot\nabla)\boldsymbol{b}, \tag{19}$$

$$\nabla \cdot \boldsymbol{v} = \nabla \cdot \boldsymbol{b} = 0, \tag{20}$$

where the subscript "0" denotes the steady state, and the lower cases denote the disturbance properties. In the neutral sheet, $\boldsymbol{B}_0 = 0$, and the small disturbance in Equations (18) and (19) are

$$\rho\Big[\frac{\partial \boldsymbol{v}}{\partial t} + (\boldsymbol{v}\cdot\nabla)\boldsymbol{V}_0 + (\boldsymbol{V}_0\cdot\nabla)\boldsymbol{v}\Big] = -\nabla\varphi - \rho v_{\rm in}\boldsymbol{v}, \tag{21}$$

$$\frac{\partial \boldsymbol{b}}{\partial t} = (\boldsymbol{b}\cdot\nabla)\boldsymbol{V}_0 - (\boldsymbol{V}_0\cdot\nabla)\boldsymbol{b}. \tag{22}$$

Assuming the plasma in the ion tail flows along the tail and adopting a narrow parabolic approximation $(\alpha \ll \beta)$ in the parabolic cylindrical coordinate, we have

$$\boldsymbol{V}_0 = V_0(\alpha,\beta,z)\tau d\beta = (0, V_0(\alpha,\beta,z), 0), \tag{23}$$

where $\tau = c(\alpha^2+\beta^2)^{1/2}$ and $\boldsymbol{e}^1 = \tau d\alpha$, $\boldsymbol{e}^2 = \tau d\beta$ and $\boldsymbol{e}^3 = dz$ are the local upper base in the parabolic cylindrical coordinate system. Because $\nabla\cdot\boldsymbol{V}_0 = 0$, Equation (23) can be written as

$$\boldsymbol{V}_0 = \Psi(\alpha, z)d\beta, \tag{24}$$

where $\Psi(\alpha,z) = \tau V_0(\alpha,\beta,z)$. We assume that there is an equal wavelength perturbation along the tail, namely the perturbation with a form

$$\boldsymbol{b}, \boldsymbol{v} \propto \exp[i(k\beta^2 - \omega t)]. \tag{25}$$

Equations (21), (22) and (20) in parabolic cylindrical coordinates can be written as

$$\rho\Big[\frac{\partial \boldsymbol{v}}{\partial t} + (\boldsymbol{v}\cdot D\boldsymbol{V}_{0i})\boldsymbol{e}^i + (\boldsymbol{V}_0\cdot Dv_i)\boldsymbol{e}^i\Big] = -\nabla\varphi - \rho v_{\rm in}\boldsymbol{v}, \tag{26}$$

$$\frac{\partial \boldsymbol{b}}{\partial t} = (\boldsymbol{b}\cdot D\boldsymbol{V}_{0i})\boldsymbol{e}^i - (\boldsymbol{V}_0\cdot Dv_i)\boldsymbol{e}^i, \tag{27}$$

$$v_1\frac{c^2\alpha}{\tau} + v_2\frac{c^2\beta}{\tau}[1 + 2ik(\alpha^2+\beta^2)] = 0, \tag{28}$$

$$b_1\frac{c^2\alpha}{\tau} + b_2\frac{c^2\beta}{\tau}[1 + 2ik(\alpha^2+\beta^2)] = 0, \tag{29}$$

where $Dv_i = dv_i - \omega_i^j v_j$ and $Db_i = db_i - \omega_i^j b_j$, $DV_{0i} = dV_{0i} - \omega_i^j V_{0j}$ and ω_i^j are 1-forms of Cartan connection forms (as mentioned above). When a lower case Latin index such as i, j appears twice in a term, summation over that index from 1 to 3 is implied.

Equations (27) and (28) may be written as

$$\left.\begin{aligned} \Big[\frac{c^2}{\tau^3}V_0\beta - i\Big(V_0\frac{1}{\tau}2k\beta - \omega\Big)\Big]b_1 &= 0 \\ \frac{1}{\tau}\Big(\frac{\partial V_0}{\partial\alpha} - \frac{c^2}{\tau^2}V_0\alpha\Big)b_1 + \frac{1}{\tau}\Big[\frac{\partial V_0}{\partial\beta} - i\Big(\frac{V_0}{\tau}2k\beta - \omega\Big)\Big]b_2 + \frac{\partial V_0}{\partial z}b_3 &= 0 \\ \Big(V_0\frac{1}{\tau}2k\beta - \omega\Big)b_3 &= 0 \end{aligned}\right\}, \tag{30}$$

$$\left.\begin{aligned} \Big[\Big(v_{in} - i\omega\Big) + \beta\tfrac{c^2}{\tau^3}V_0 + V_0\frac{1}{\tau}2ik\beta\Big]v_1 - 2\frac{c^2}{\tau^3}\alpha v_2 &= 0 \\ \frac{1}{\tau^2}\frac{\partial\Psi}{\partial\alpha}v_1 + \Big(v_{in} - i\omega - \frac{c^2}{\tau^3}\beta V_0 + V_0\frac{1}{\tau^2}2ik\beta\Big)v_2 + \frac{1}{\tau}\frac{\partial\Psi}{\partial z}v_3 + \frac{1}{\tau\rho}2ik\beta\phi &= 0 \\ \Big(v_{\rm in} - i\omega + \frac{1}{\tau}V_0 2ik\beta\Big)v_3 &= 0 \end{aligned}\right\}. \tag{31}$$

From Equation (30) and $\alpha \ll \beta$, hence we have the dispersion equations

$$\left.\begin{aligned} \omega_1 &= V_0 \frac{\beta}{\tau}\Big(2k + i\frac{c^2}{\tau^2}\Big) \approx 2k\frac{V_0}{c} + i\frac{V_0}{c\beta^2} \\ \omega_2 &= \frac{V_0}{\tau} 2k\beta + \frac{i}{\tau}\frac{\partial V_0}{\partial \beta} \approx 2k\frac{V_0}{c} - i\frac{V_0}{c\beta^2} \\ \omega_3 &= \frac{1}{\tau} 2k\beta V_0 \approx \frac{1}{c} 2kV_0 \end{aligned}\right\} . \tag{32}$$

For ω_2 and ω_3, the motion of the plasma in the neutral sheet is steady, but not steady for ω_1. At this time, $b_3 = 0$, $b_1 \neq 0$ and $\frac{b_2}{b_1} = -\frac{\partial V_0/\partial\alpha - (c^2/\tau^2)V_0\alpha}{\partial V_0/\partial\beta - (c^2/\tau^2)V_0\beta}$ can be obtained from Equation (30).

In the neutral region composed of the cometary magnetic cavity and the neutral sheet (Liu 1999), the motion of cometary plasma cannot be influenced by solar wind and interplanetary magnetic fields. The ions move at $\sim 1\ \mathrm{km\,s^{-1}}$, the same velocity as those from the neutral molecules going through sublimation from the nucleus. Therefore, in the neutral sheet of the ion tail, cometary ions move toward the tail direction with a low uniform speed (Baker et al. 1986; Richardson et al. 1986). Hence, $\frac{\partial V_0}{\partial \alpha} = 0$ and $b_2 \ll b_1$.

The instability of the plasma with $b_1 \neq 0$ shows that there exists an enlarged disturbance perpendicular to the tail direction. This argument has been demonstrated by the observation of Comet G.-Z, when the ICE spacecraft was flying through its the tail.

4 DISCUSSION

From Equation (28), it is not difficult to see that the growth rate of instability is $V_0/c\beta^2$. From Equation (17), we find that as the distance to the nucleus becomes longer (the larger β^2 is), the growth rate becomes smaller. Therefore, the growth rate is very large near the head of the comet in the neutral sheet. Once the small disturbance occurs, the magnetic field of the disturbance is quickly amplified. If the amplified magnetic field can penetrate the magnetic pile-up region outside the neutral sheet, a magnetic field nearly perpendicular to the tail axis can be added to the steady magnetic field which is nearly parallel to the tail axis and makes the local magnetic field structure of the tail near the cometary head of the comet change. This may be one of the reasons that explains the formation mechanism of the tail rays. Ershkovich et al. (1986) considered the effects of the coupling between the plasma and neutral particles on the stability of the ion tail and folding comet rays, and found that the cometary rays were subject to both stabilizing and destabilizing effects because of the drag from neutral ions. Regarding why there are time intervals in the ray generation, further discussions are needed.

Here we briefly remark about the Liu's operator. Using the exterior differential operator $d = \nabla\wedge$ connected to vector algebra and vector analysis, it gives grad, div and rot. Liu's operator and its associated method have solved the operation $(\boldsymbol{A}\cdot\nabla)\boldsymbol{B}$ in exterior differentiation and derived the possible formulas of vector analysis. Only the exterior differential operator d cannot solve these problems. Using the operator D, we simplify the vector analysis method and obtain results which cannot be derived in vector analysis, i.e. the expression of $(\boldsymbol{A}\cdot\nabla)\boldsymbol{B}$ in an orthogonal curved coordinate system. This expression is very important for the study of stability in hydrodynamics and magnetohydrodynamics. It may be used to study the stability of cometary plasma and local structures on the solar surface (e.g. nearby a sunspot), as long as the collection of magnetic lines can be approximated as a particular curved coordinate system.

Acknowledgements We would like to acknowledge the support of the National Natural Science Foundation of China (NSFC, Grant Nos. 10573037, 10778637, 10933004 and 11003048), the Minor Planet Foundation of Purple Mountain Observatory and the exchange program between the Finnish Academy (FA) and NSFC.

References

Alfvén, H. 1957, Tellus, 9, 92

Baker, D. N., Feldman, W. C., Gary, S. P., et al. 1986, Geophys. Res. Lett., 13, 271

Biermann, L. 1951, Zeitschrift für Astrophysik, 29, 274

Biermann, L., Brosowski, B., & Schmidt, H. U. 1967, Sol. Phys., 1, 254

Cravens, T. E. 1986, in Proc. 20th ESLAB Symp. on the Exploration of Halley's Comet, Vol. I, ed. B. Battrick (ESA SP-250) (ESA: Noordwijk), 241

Ershkovich, A. I., & Flammer, K. R. 1988, ApJ, 328, 967

Ershkovich, A. I., Flammer, K. R., & Mendis, D. A. 1986, ApJ, 311, 1031

Ershkovich, A. I., & Israelevich, P. L. 1993, ApJ, 411, 891

Ershkovich, A. I., McKenzie, J. F., & Axford, W. I. 1989, ApJ, 344, 932

Ershkovich, A. I., & Mendis, D. A. 1986, Earth Moon and Planets, 36, 127

Gloeckler, G., Allegrini, F., Elliott, H. A., et al. 2004, ApJ, 604, L121

Gloeckler, G., et al. 2000, Nature, 404, 576

Hansen, K. C., et al. 2007, Space Sci. Rev., 128, 133

Ip, W.-H., & Axford, W. I. 1987, Nature, 325, 418

Ip, W.-H., & Axford, W. I. 1990, in Physics and Chemistry of Comets, ed. F. Huebner (Berlin: Springer), 177

Jones, G. H., Balogh, A., & Horbury, T. S. 2000, Nature, 404, 574

Liu, L.-Z. 1999, ApJ, 520, 399

McKenzie, J. F., Axford, W. I., & Ershkovich, A. I. 1990, ApJ, 360, 275

Neubauer, F. M., et al. 1986, Nature, 321, 352

Neubauer, F. M. 1990, in Comet Halley: Investigations, Results, Interpretations, 1, 79

Neugebauer, M., et al. 2007, ApJ, 667, 1262

Richardson, I. G., Cowley, S. W. H., Hynds, R. J., et al. 1986, Geophys. Res. Lett., 13, 415

Riley, P., Gosling, J. T., McComas, D. J., & Forsyth, R. J. 1998, J. Geophys. Res., 103, 1933

Slavin, J. A., Smith, E. J., Tsurutani, B. T., et al. 1986, Geophys. Res. Lett., 13, 283

Wallis, M. 1971, Nature, 233, 23

Wegmann, R. 2002, A&A, 389, 1039

Westenholy, C. Von, 1981, Differential Forms in Mathematical Physics, revised edition (Amsterdam: North-Holland)